LASER INTERFEROMETER GRAVITATIONAL WAVE OBSERVATORY

LIGO Laboratory / LIGO Scientific Collaboration

LIGO-T070080-00 *ADVANCED LIGO* 04/03/2007

HAM-SAS Prototype
Installation and Commissioning Experience

Riccardo Desalvo

Distribution of this document:
LIGO Scientific Collaboration

This is an internal working note
of the LIGO Laboratory.

California Institute of Technology
LIGO Project – MS 18-34
1200 E. California Blvd.
Pasadena, CA 91125
Phone (626) 395-2129
Fax (626) 304-9834
E-mail: info@ligo.caltech.edu

Massachusetts Institute of Technology
LIGO Project – NW17-161
175 Albany St
Cambridge, MA 02139
Phone (617) 253-4824
Fax (617) 253-7014
E-mail: info@ligo.mit.edu

LIGO Hanford Observatory
P.O. Box 1970
Mail Stop S9-02
Richland WA 99352
Phone 509-372-8106
Fax 509-372-8137

LIGO Livingston Observatory
P.O. Box 940
Livingston, LA 70754
Phone 225-686-3100
Fax 225-686-7189

http://www.ligo.caltech.edu/

Introduction

This report details the identification and resolution of problems encountered in the commissioning of the HAM-SAS prototype. It serves as a record of changes that were implemented in the design, or that should be implemented in future production. It is a companion to the report to the HAM-SAS evaluation committee which responds to the committee's charge, T070079.

In addition to the author of this report the following people have made significant contributions to the installation, commissioning, modeling or understanding of the HAM SAS prototype: Ben Abbott, Yoichi Aso, Mark Barton, Dennis Coyne, Valerio Boschi, Carlo Galli, Gianni Gennaro, Yumei Huang, Jameson Quave, David Ottaway, Virginio Sannibale, Alberto Stochino , Chiara Vanni, Hiro Yamamoto and Sany Yoshida

List of corrections implemented or identified with the Prototype and to be implemented in Production

HAM SAS is a seismic isolator supporting the existing optical benches in the Advanced LIGO HAM chambers. It is designed to provide the isolation performance of HEPI plus ISI in a single stage through mostly passive means.

The HAM SAS design was first presented at the Amaldi-6 conference in the summer of 2005. Prototype fabrication was approved to start in April 2006. The finished unit was delivered in Boston at the end of December 2006. Installation and commissioning in a LASTI HAM chamber started in January 2007.

The HAM SAS design includes development of in-factory production, UHV cleaning, baking, clean-room assembly and tuning procedure, thus sparing scarce LIGO manpower and premises. These operations were all performed at Galli & Morelli in Lucca, Italy. Part of the tuning of this prototype was done in LASTI because G&M did not have a HAM bench available as payload but at least two more optical benches will have to be built and the full tuning of subsequent production items is expected to be performed in-factory.

The following is a partial and in part random order list. Some actions, like for example repositioning bolting patterns to improve and speed-up construction, are included in the design update or listed elsewhere

1 Welding problems

During construction we encountered severe problems in performing aluminum welding. Our original weld design would produce cavities and introduce unacceptable warping in the weldments. To avoid these problems, in collaboration with G&M and Technoinox, we developed heat-flow-optimized geometries that reliably avoided formation of cavities, as well as counter-stressing and annealing techniques that virtually eliminated warping. We also redesigned and replaced all

weldments that could not be built with sufficient precision and cleanliness with machined and bolted structures. Incorporation of the welding techniques and weld preparation details from the initial LIGO seismic isolation effort performed by Allied Engineering and Production Corporation could have mitigated the problems considerably.

The welding problems were encountered in the production of the base structure, the developed solutions now allow reliable production of these structures, including additional optical benches, which use the same type of welding.

The gathered know-how has been useful in advising on welded fabrication of the SUS frame structures.

Other welding problems were encountered in building the LVDT and actuator support structures. These weldments structures were completely replaced with machined structures.

These unforeseen developments, re-design, part replacements and unexpected assembly variations induced substantial additional costs and several months of construction delay but, according to G&M and to our own estimations, will not significantly increase the construction costs or construction time of further production items.

The tilt instability problem

During assembly we encountered an unanticipated optical bench tilt instability problem, missed by all our simulations. The problem derived from the fact that the c.o.m. of the optical bench and its payload is above the supporting GAS filters and effective bending point of the resulting structure. The table is in unstable equilibrium. Stable equilibrium was recovered with the introduction of a rapidly designed and built roll bar connected to a star of 4 springs that restored a concave potential. This modification added a small additional delay to the construction schedule and was not tested in the factory to avoid larger delays.

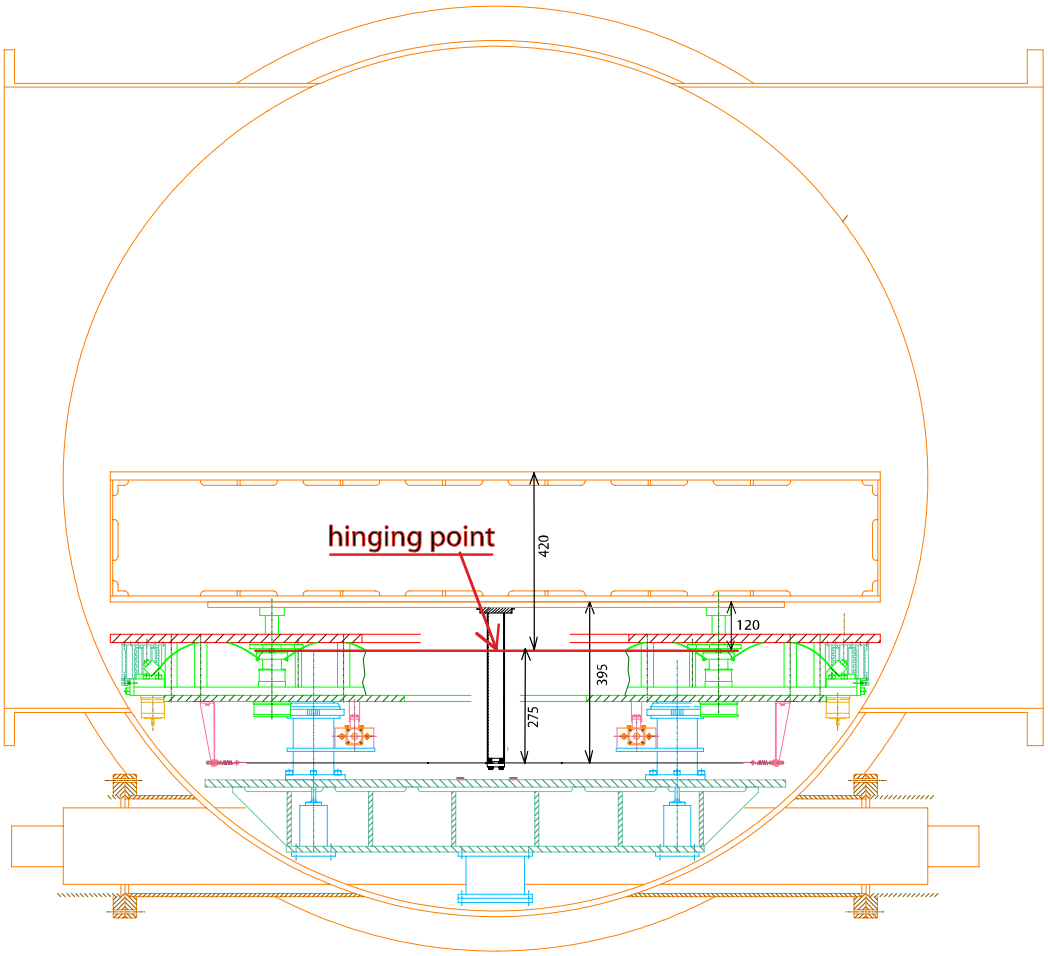

Figure A3-1. Schematic of the Tip & Tilt Stabilization Assembly

A much worse damage to the schedule came during commissioning at LASTI because, after UHV cleaning, the roll bar bolt was not properly tightened and tilt instability ensued. We lost almost a month of commissioning time because we initially though that we had underestimated the required stiffness of the 4 springs and we wasted time in ordering, UHV processing and trying out several sets of springs before we made the correct diagnosis and fix the problem. Even after diagnosing the problem, we realized that the roll bar was encased in the set of witness LVDTs and almost unreachable. We had to assemble and clean a “long” and “sneaky” wrench to finally solve the problem and resume commissioning. In future versions a monolithic roll bar and flange will be used rather than a cinched clamp arrangement.

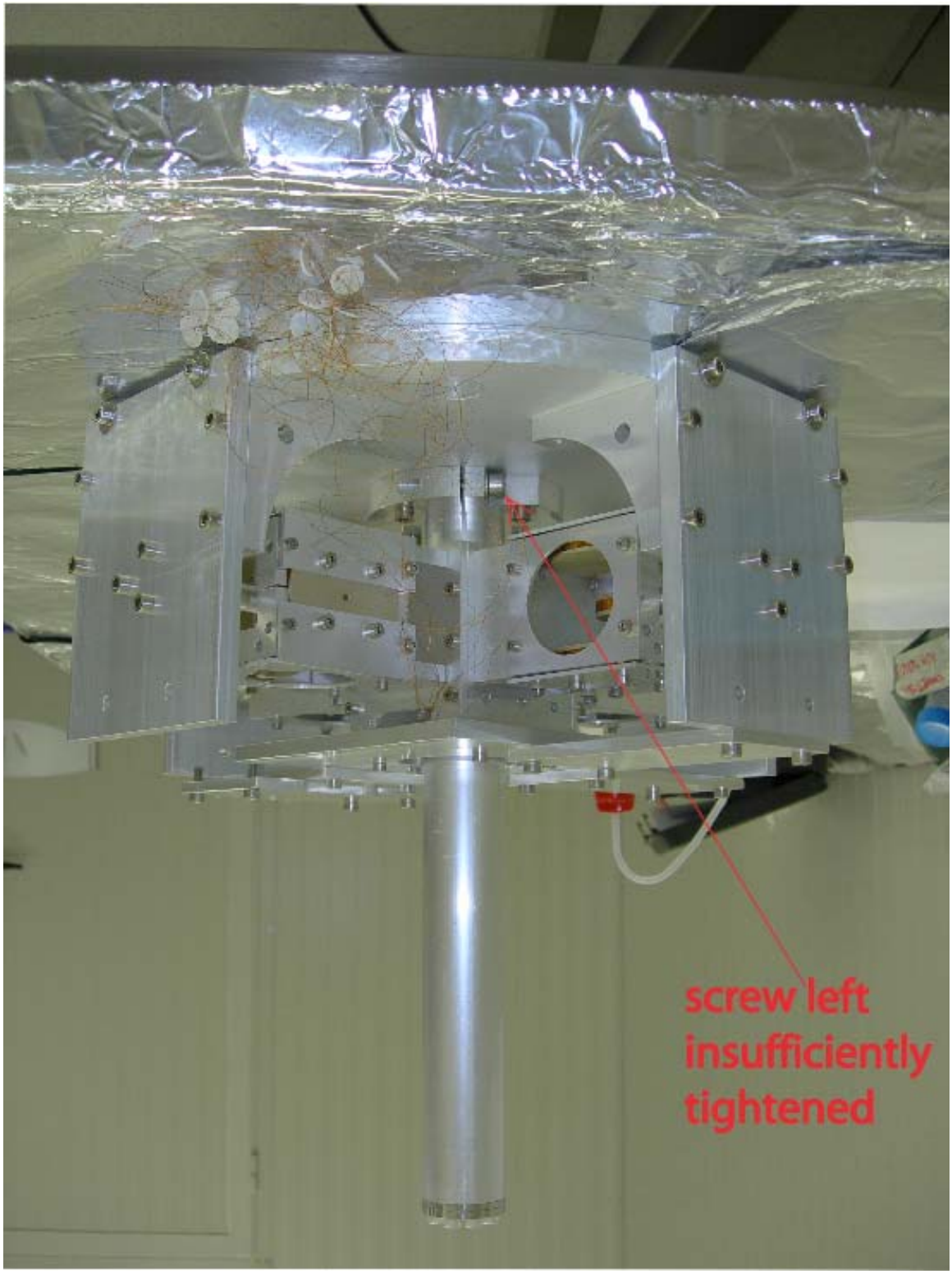

Figure A3-2. The plate, carrying the four witness LVDTs bolts below the center of the optical bench, in between of the four GAS filters. View of and access to the bolt is mainly obscured by the GAS blades and other structures.

Cleaning, baking and assembly infrastructure.

The tight Advanced LIGO UHV requirements demanded special cleaning and baking procedures. All steps of cleaning procedures were carefully vetted by LIGO personnel and approved. To perform these procedures:

A cleaning facility was built at P. Soldi (a long term G&M subcontractor).

A large (3 m diameter, 1.2 m height) UHV compatible stainless steel 200^{c}C baking oven was designed and built to process both the large parts before assembly and the final assembled and tuned SAS unit. The oven used a nitrogen atmosphere derived from LN2 boil off.

A similar performance, 250^{o}C small and rapid cycling oven was built to process small components.

A large clean room adjacent to a large grey room were built for the SAS assembly.

Clean-room-grade handling equipment to move, support and position the parts during assembly were built

Numerous FTIR tests were performed both at G&M at suitable construction stages and at LASTI after delivery.

Non-recurring facility investment costs were absorbed by G&M (e.g. clean room air handling), while LIGO contributed non-recurring engineering costs for the specialized handling equipment (~$30k) and the baking ovens (~$51k).

The knowledge and facilities developed are now available for production and are presently in use for cleaning and baking the large parts of the BSC-ISI prototype.

Material and parts cleaning procedures.

Stainless steel was washed, etched, most parts electropolished, neutralized and washed

Aluminum underwent basic etching and scrubbing, acid etching (more than one cycle when necessary)

Maraging and soft iron where etched before plating, then neutralized and washed

After etching or plating, all of the metal parts rinsed with de-ionized water and dried before baking, which was performed in a similarly cleaned stainless steel oven in boil-off nitrogen atmosphere at 200^{o}C for a day (plus a day of ramp-up and one of ramp-down).

The NdFeB magnets, all of the SH alloy, bakeable up to 150^{o}C were washed in warm alcohol and ultra sound for 30 minutes, then baked to 135 degrees.

Peek was treated like the NdFeB magnets before coiling.

OHFC copper is used in wiring, most comes pre-coated in Kapton.

The coil wiring is wound in clean conditions (the coiler spools where cleaned and the coiler wrapped in aluminum foil) and then washed in warm alcohol and ultra sound for 30 minutes before painting with polyimide resin (for immobilization).

The polyimide resin was thermally polymerized with its require temperature profile, then kept at ~200 degree for a day for outgassing.

Final baking and shipment.

The fully assembled and tuned SAS unit undergoes final re-bake for added cleanliness and for creep burnout just before packaging and shipping. The aluminum foil and clear plastic packaged assembly (according to LIGO UHV procedures) is then further enclosed in an in-situ welded air tight bag, provided with a filtered breathing opening and silica gel humidity traps, crated and air-shipped to the US. Suitably cleaned (class B) handling equipment, necessary to move, handle and position the SAS unit, is similarly packaged and shipped in separate crates. The many lessons learned make the system more reliable, faster and easier to build and assemble.

Polyimide resin potential problem.

HAM SAS is instrumented with LVDT sensors and voice coil actuators. To guarantee full UHV compatibility, and avoid any risk of crippling leaks (or virtual leaks) from sealed instruments, both instruments are made with passive coils directly exposed to vacuum. The only insulating materials that we allowed are Kapton, Polyimide resin and PEEK.

PEEK is used as material for the spools that support the wires. Kapton insulated wires are used for coiling, polyimide resin is painted on the actuator coils for rigidity and allow precision actuation at high frequency. The high temperature characteristics of the two materials, and the coil power supply limitations, impede in-vacuum overheating (the only dangerous failure mode).

During the coil production we encountered an unexpected UHV compatibility question of the polyimide resin. During polimerization the polyimide precursor emits gas, which diffuse out of the resin. We normally put some resin on an aluminum foil to polimerize next to the coil. We noticed that while thin films polimerize in a thin, compact and transparent film, places on the aluminum foil where the polyimide was thicker than a critical value of about half millimeter the resin tends to “foam” during polimerization. The foam is a whitish, very brittle and very light foam with pores much smaller than a millimiter.

This can be a very serious problem not only because the foam traps polimerization gases, but also because cracked pores are perfect receptacles for any kind of dirt. This may be a common problem for any place in Ad-LIGO where polyimide resin is used (OSEMs, other actuator coils, etc.). The worry is that resin can flow or be wicked in spaces behind the wire, where volumes can be partially filled with sufficient resin to support foaming.

After identifying the problem (with test coils) we mitigated it by not using the resin unless absolutely necessary (for example we did not use it in the circular LVDT coils where the wire tension is sufficient to make a solid coil), checking for possible places where the resin can accumulate (luckily the small gauge wire allows for empty volumes smaller than the critical foaming size), and stretch the rampup time around the polimerization temperature to allow the maximum gas diffusion (we observed that this reduced the foaming). While we are confident that

the HAM SAS actuator coils are well compatible with the LIGO UHV specifications, we are developing a safe procedure for all Ad-LIGO.

The Horizontal Actuator Wiring Shearing Accident.

The sensor and actuators are arranged in collocated units. The units are modular and are pre-assembled before installation on the SAS unit. The coils are robust and do not break down, unless hit directly. The cabling is more delicate. We simply extended the coil wire in the form of a twisted pair, and crimped the wires into an Accuglass sub-D connector.

The thin gauge wiring is exposed and has a potential for damage if a tool or a finger snag them.; Some further work on securing or routing the coil wires to minimize the risk is needed.

When we replaced the weldment LVDT/actuator supports we accidentally made two edges that interfered before the horizontal end stops interrupted the movement end (the actuator magnet yoke acted as an end stop for the IP, against the new LVDT support). For bad luck one of the actuator coil twisted wire was caught in between and sheared. This happened in the LVDT along the beam line, in the least accessible unit, between the two support cross tubes.

Despite the awkward position we managed to dismount the coil and repair the wire in place, without having to extract the SAS from the HAM chamber (by using the electrical feedthrough port).

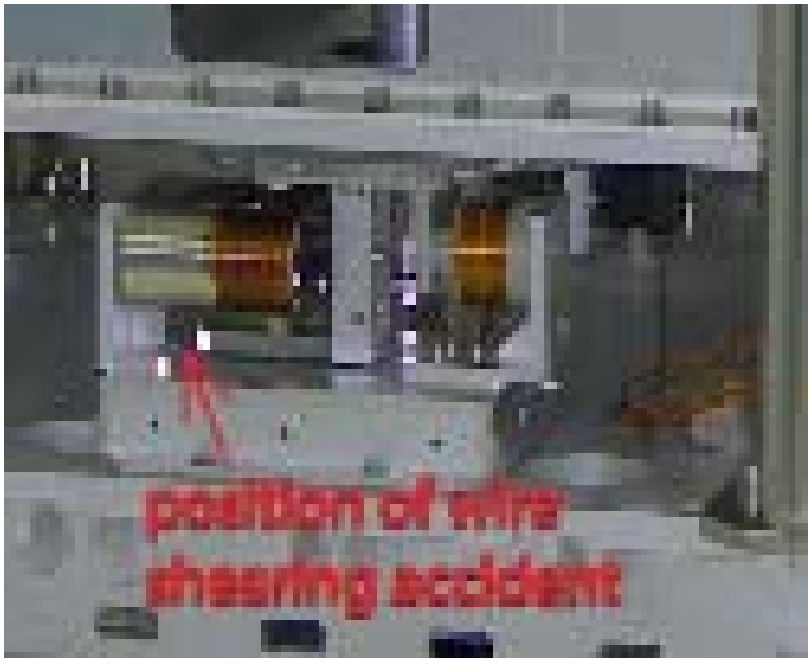

Figure A3-3. Position of accidental shearing of wire. The clearance present in the original weldments became an interference in the UHV clean assembly and sheared one of the actuation coil twisted pairs. This photo was taken before the unit was lowered inside the HAM chamber. The broken actuator ended up buried along the HAM beam-line which complicated the repairs.

Redesigned support and end stops.

The lesson learned suggested a small modification of the bolting of the horizontal sensor/actuator unit that will allow replacement of the entire unit or parts of it without major work. Also an Accu-Glass-like connectoring on each coil will allow easy replacement of each coil as well as simpler and sturdier cabling.

Additionally, nulling the LVDT signal at the IP working position was found to be not easily feasible with the present configuration. Slotted holes in the LVDT stand and a pushing screw will allow nulling of the LVDT signal at the IP nominal working point as it is done already for the vertical direction. This tuning would be done in the factory.

The 90 degree symmetry of the SAS vacuum chamber required the installation of 4 sensor/actuator pairs for both the three horizontal and for the three vertical degrees of freedom. This instrumentation symmetry allows for an easy diagonalization when all pairs are operational.

The coils are expected to be quite failure resistant since the coil currents are not high enough to cause significant heating. Nevertheless the redundancy of 4 sensor/actuator pairs per three degrees of freedom allows the system to function even in case of failure of one sensor and one actuator in the vertical and/or the horizontal groups of degrees of freedom, although with a more difficult diagonalization. Indeed for several days before the horizontal actuator was repaired, we operated with three actuators only and still managed DC control of the IP.

The only problem worth mentioning in the vertical sensor/actuator units is that a warped top plate forced one of the GAS filters to work slightly crooked. The tip of the actuator coil moved more than its 2.5 mm clearance and ended up scraping on the magnet yoke. We had to use the play of the support screws to generate a half mm play and correct functioning. The problem has no practical consequences and will be corrected in a more professional way if and when the SAS system will be overhauled.

No modification is suggested for the vertical direction sensor/actuator units (with the exception of the Accu-Glass-like connectoring) because they are already easy to assemble and disassemble and already include a suitable signal nulling mechanism.

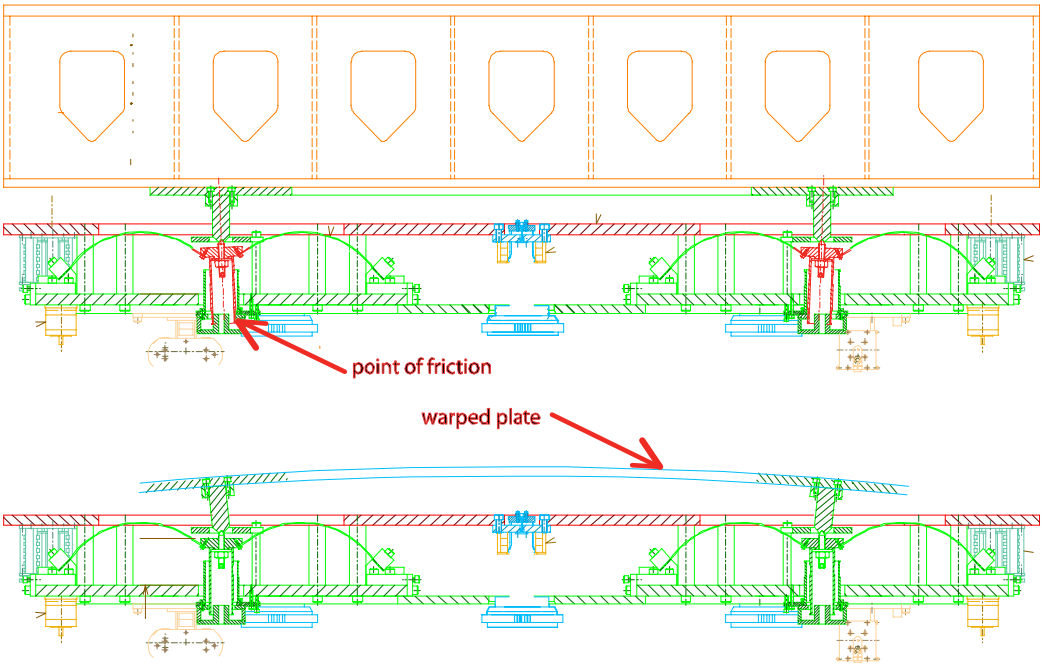

Figure A3-4. Illustration of the warped cable problem.

Insertion of the SAS module into the HAM chamber

Access into the HAM chambers is more difficult than in BSC chambers because one cannot use the bridge crane. We designed an insertion tool allowing the installation of a fully-assembled SAS module and of its optical bench into a HAM chamber. The machinery consists of two elevator carts positioned on both sides of a HAM chamber, connected by two rails. One elevator cart is mounted between the pier and the HAM chamber, close to the HAM door, the other elevator is 3 m away from the other HAM door.

The elevators can raise the rails to allow the SAS module, or the optical bench, to slide underneath. The rails are then lowered to attach to their payload. The elevators then lift the payload above the pier and the door obstructions until it can be pushed inside the HAM chamber. The HAM module is then lowered on the support tubes and bolted down.

Next the optical bench is lifted and pushed in operation. Since the (old) optical bench simply sits over the SAS module top plate, the insertion procedure can be done completely with horizontal movements (the SAS module is pre-compressed below its working point and then released once the Optical bench has sled in place).

This installation procedure successfully inserted the SAS module and its optical bench into the HAM chamber. We found that the system has a tendency to lean towards or away from the chamber and some outrigging or stiffening of the elevator as well as some stiffening of the rails are needed. We also found that it would be convenient to have longer rails and move the inner elevator on the external side of the piers. This would make the rail heavier and relatively more flimsy, thus requiring even more stiffening. At present the individual rails are light enough that two persons can handle them and insert in or remove them from the HAM chamber. A longer and stiffer

(heavier) rail would require crane insertion, an operation possible at the sites (impossible at LASTI for lack of overhead crane on the clear side of the HAM). Apart these minor changes the technique worked as planned allowing the optical bench to be inserted fully populated.

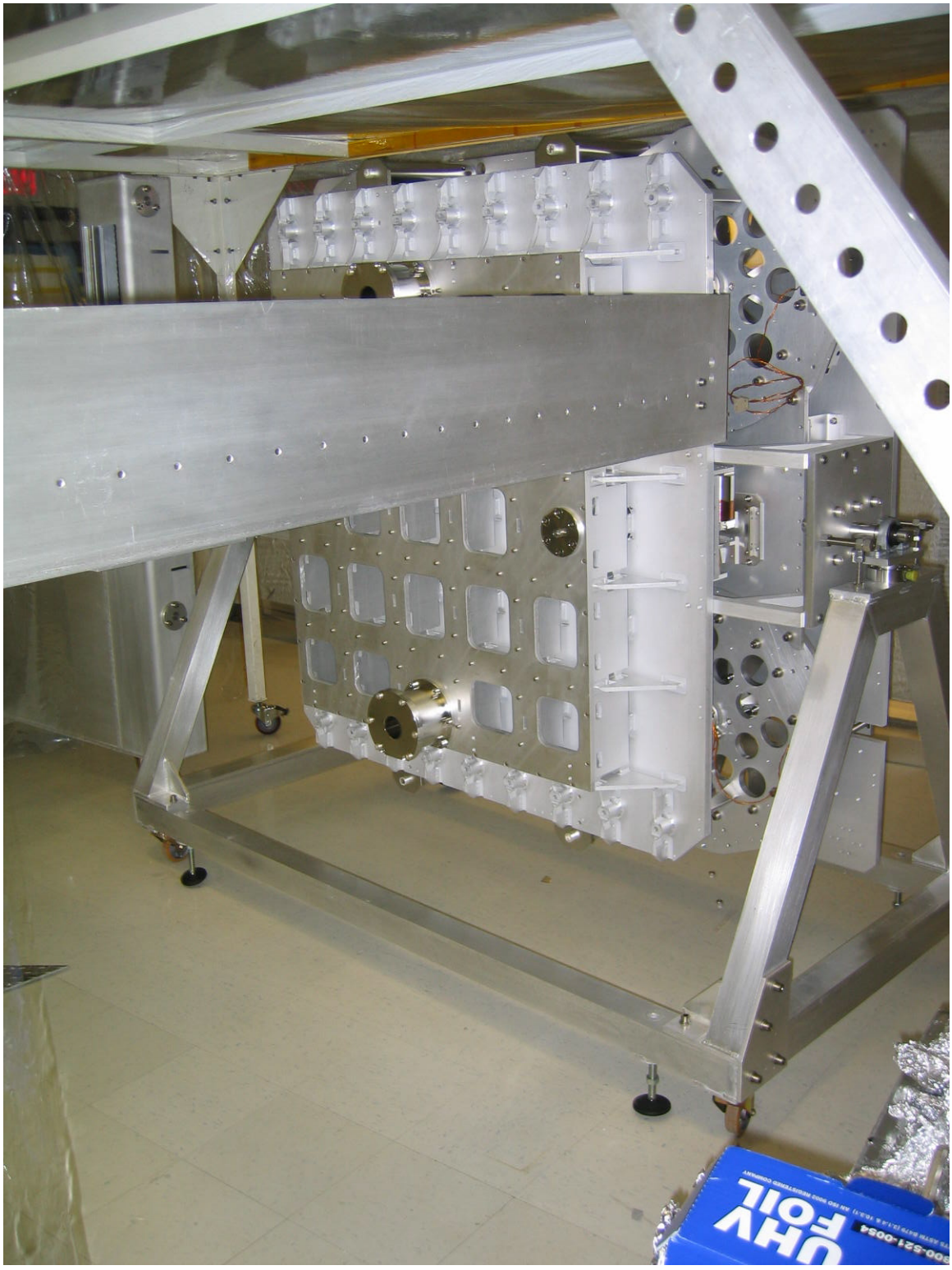

Figure A3-5. The Ham structure on its transport cart, still tilted at 90^{o} to pass through doors, is presented in front of the installation rails. For local space reasons we were forced to temporarily remove the elevator cart on the access side to allow access to the cart first for the SAS structure, and then for the optical bench. In the observatories, where the necessary space is available, the cart is expected to simply roll under the rails..

Figure A3-6. Elevator/insertion structure in the G&M grey room, before packing and shipping. The rails are lifted by turning the cranks, one of which is visible in the foreground.

Freezing the optical bench in space for access and maintenance.

In the horizontal plane we use “crown” screws (red in the drawing) threading on the O.D. of the IP leg protection tubes (light blue). Raising the crown screws, they engage in a hole in the SAS spring box plate (green) and freeze it in place in the horizontal direction (split drawing on the right side of the leg). When retracted (split drawing on the left side of the leg) the leg protection pipe still provide the end stop for the IP movement. A range limiting ring (black) was introduced at LASTI to reduce the IP movement range (from 10 to 5 mm), to eliminate the interference problem with the replacement LVDT/actuator supports.

Four “crown” screws are available, one each on the four IP legs, but two only, the two easily accessible ones from the two HAM doors, are necessary and more than sufficient to immobilize the spring box.

These screws freeze the movement of the IP around its mechanical centered position.

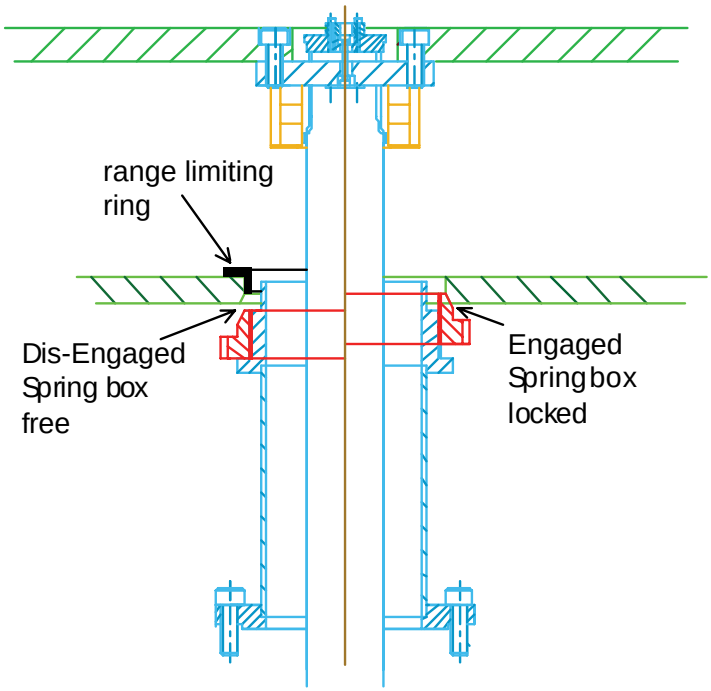

Figure A3-7. Illustration of the “crown” screw action in locking the horizontal movement. Disengaged on the left and engaged on the right.

Four clamps mounted in cantilever from the edges of the spring box were added to freeze the vertical movement of the optical bench around its working point with a precision of a fraction of a millimeter. With the two crown screws and the four clamps locked, the table is solid enough that we walk or crawl over it without consequences. We have found that occasionally, when hitting the aluminum range limiting ring, the IP movement sticks. We expect to eliminate this occasional problem by using stainless steel for the contact surfaces rather than aluminum.

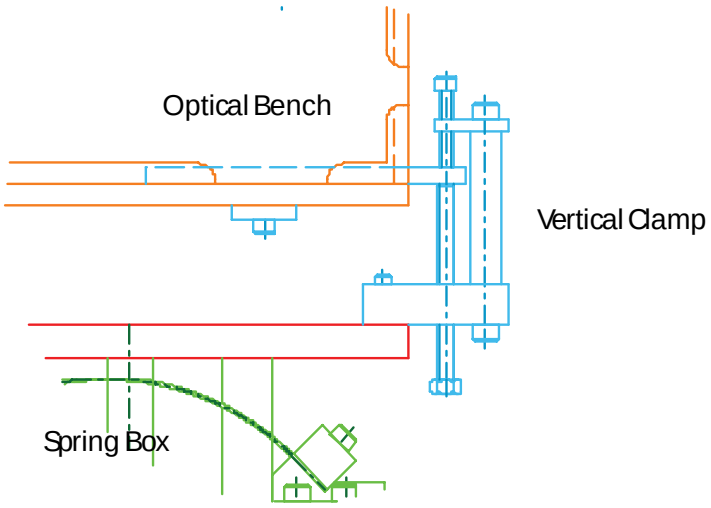

Figure A3-8. Sketch of the external clamps added at LASTI to lock the optical bench in the vertical direction. The four clamps are mounted between the spring box (one GAAS spring visible) and the optical bench itself. The two screws in each clamp are retracted 10 mm in operation.

Control work and strategies

HAM SAS is basically a passive system. It provides the bulk of its performance passively. Nevertheless all SAS degrees of freedom are equipped with collocated position sensors (LVDT) and voice coil actuator pairs for position controls, damping of resonances and performance.

These sensor/actuator pairs have three main functions:

- Static controls, to position the table and to compensate for thermal, tidal and slow tilt drifts
- Resonance damping, to reduce the r.m.s. residual motion of the table.
- To provide electromagnetic springs in parallel to the GAS springs and the IP, to control and minimize the mechanical resonant frequencies.

As an optional extension of the SAS concept, the actuators can be used in feed-forward from ground seismometers to further reduce residual motion. An additional option, for future upgrades, could involve feedback from onboard accelerometers, assuming that an accelerometer with suitable sensitivity can be implemented

The static controls are represented by a slow integrator (response time of a mHz or less) that for each degree of freedom generates a quasi static current in the control coils. Although we have seen that there is no need for a faster correction (the integrator was holding the table in position even with the faster in-air temperature fluctuations) this signal can be used to slave the table to any external signal (global controls, SPI, etc.). Any significant control force with characteristic time longer than a day (subsidence, seasonal tilts, seasonal temperature changes, large changes of floor loading) are offloaded by the stepper-motor-actuated auxiliary tuning springs, in the same way used to balance the tilt floor caused by pumpdown.

Only weak damping of the resonances is necessary to eliminate the problem of enhancement of the ground slow motion movements. This is done by providing a viscous force at each resonant

frequency, on each degree of freedom and the roll if off at higher frequency. Only few degree of freedom, and maybe none, may need this damping.

The electromagnetic spring used to lower the mechanical resonant frequency of the different degrees of freedom is a key feature of the passive attenuation mechanism. It is basically the same mechanism that allows the low frequency sensitivity inside the STS2 and all electrically softened seismometers. By lowering the resonant frequency one shifts to lower frequency the $1/f^2$ attenuation curve of the mechanical oscillator. We count on driving all resonances close to, or below, 30 mHz to provide sufficient attenuation at the microseismic peak[1]. We have already achieved 10 mHz resonance in the vertical mode, arguably the most difficult. This operation, though, is a delicate one. The e.m. spring has to be applied in a modal mode, which require a good diagonalization. At high frequency the diagonalization is easy, for example the sum of all vertical sensor is the vertical degree of freedom, and the differences give the tilts. At low frequency it is more difficult. Basically low frequency is obtained by nulling strong contributors of different sign (the mechanical spring and antispring). The closer one gets to zero frequency, the more small differences become important. Little differences in thickness of the blades on the two sides of the blades mix some tilt in the vertical mode. This has to be characterized and corrected with the e.m. springs. The characterization step is the slow step. Frequency sweeps, or even white noise measurements below the mHz take many hours and are prone to corruption by accidental perturbations. Once characterized and well diagonalized, though, the system is expected to be stable and to require no maintenance because creep in the system springs have been burned out by the final baking step. Since the quality factor of any mechanical resonance falls with the square of the frequency[2], with sufficient diagonalization to drive of all vertical degrees of freedom below 30 mHz there would be no residual need for resonance damping (as observed already when we tuned the vertical movement to 10 mHz). In the horizontal degree of freedom this regime would be reached below 1o mHz, also a reasonable target.

The main figure of merit in actively controlled systems is the frequency ratio between the motion resonant frequency and the first plant internal frequency. In this measure the soft joints of HAM SAS make it a particularly favorable and well-designed system for active controls. The actuators have much more feed-forward authority (more than a N) and frequency response than the force necessary to contrast the residual seismic power (~μN or less) that may leak through the low frequency flex joints.

The SAS optical table is essentially a glorified seismometer that can reach attenuation performances similar to a seismometer sensitivity. Although there is no foreseen need (or advantage) for seismometer feedback, one could conceivably develop sufficiently sensitive

---

[1] In the first installation at LASTI, for schedule reasons and for prudence reasons (having a somewhat stiffer system at first pumpdown) we did not tune the mechanical plant at the lowest possible frequency, requiring more authority than necessary from the e.m. springs. This load can be reduced, if necessary, adding small additional mass on the spring box for the horizontal direction, and with more tuning for the vertical.

[2] Basically the loss energy, the area of any hysteresis cycle, does not depend on the cycling speed of the system, while the kinetic energy is proportional to the square of the frequency. Since the quality factor is the ratio of the loss/cycle divided by the kinetic energy, the quality factor must fall with the square of the frequency. When the quality factor becomes comparable to unity, the system becomes hysteresis dominated (stops oscillating), and the mechanical oscillator $1/f^2$ falloff turns into a 1/f behavior. The frequency at which the system transits from one slope to the other depend on the intrinsic loss of the material and on the total energy stored in the flex joint in each cycle.

seismometers (with advanced FS flex joints) to be of use for future needs. The actuators have sufficient performance for this possible advance.

Parasitic positioning springs and voice coil actuators

The static positioning of the optical bench is controlled by parasitic springs attached between the base structure and the spring box for the horizontal degrees of freedom, and between the spring box and the optical bench for the vertical degrees of freedom. The support point of these springs is on a micrometrically driven sled, controlled by UHV stepper motors. The minimum step is 5 micron[3], which multiplied by the 2 x 410 N/m stiffness of the springs means that the voice coil static load can be reduced to below 4 mN force level, less than 0.1% of its authority and 10^{-6} of its peak power (few μW).

Corrections for tidal motions and daily temperature variations are left to the voice coils. For the horizontal a tidal motion of 100 microns would require 7 mN/coil with the present tuning to 50 mHz. In the vertical direction the bulk of the deviation comes from the thermal variation of the Young's modulus ($3\ 10^{-4}/^{o}$C). We have observed that the vertical controls kept the optical bench at its nominal position using 0.65 V from the coil drivers (saturation is at 22 V) to compensate a temperature change of 0.2^{o}C (measurement taken with doors open). The measurement did not allow a good temperature-to-voltage measurement because the thermometer was in a different location in the room. Compensating for a thermal variation of 1^{o}C in the room would require a few tens of mW from the in-vacuum coils.

The graph attached illustrates the stability of the HAM SAS in the two days just after pumpdown. The vertical degrees of freedom are left free to drift during swept sine transfer function measurements, while a slow integrator feedback keeps the horizontal degrees of freedom nailed.

In the first day the vertical degrees of freedom can be observed to thermalize after the cooling from the adiabatic expansion of air during pumpdown. The vertical excursion during the first day was 0.8 mm (~0.2 micron/count) while the tilt was ~170 micro-radians in the Y direction and ~700 micro-radians in the X direction. The daily cycle can be observed after the first day.

Of course the coil actuators would have been more than sufficient to keep these positions nailed if the integrators had been switched on.

The horizontal degrees of freedom of course remain stable, even during repeated accesses to install optical levers, their cabling below the HAM chamber, removal of all the leftover ballast from the neighborhood, and other intrusions.

[3] This evaluation is carried for the horizontal direction, the numbers are quite analogous in the vertical direction.

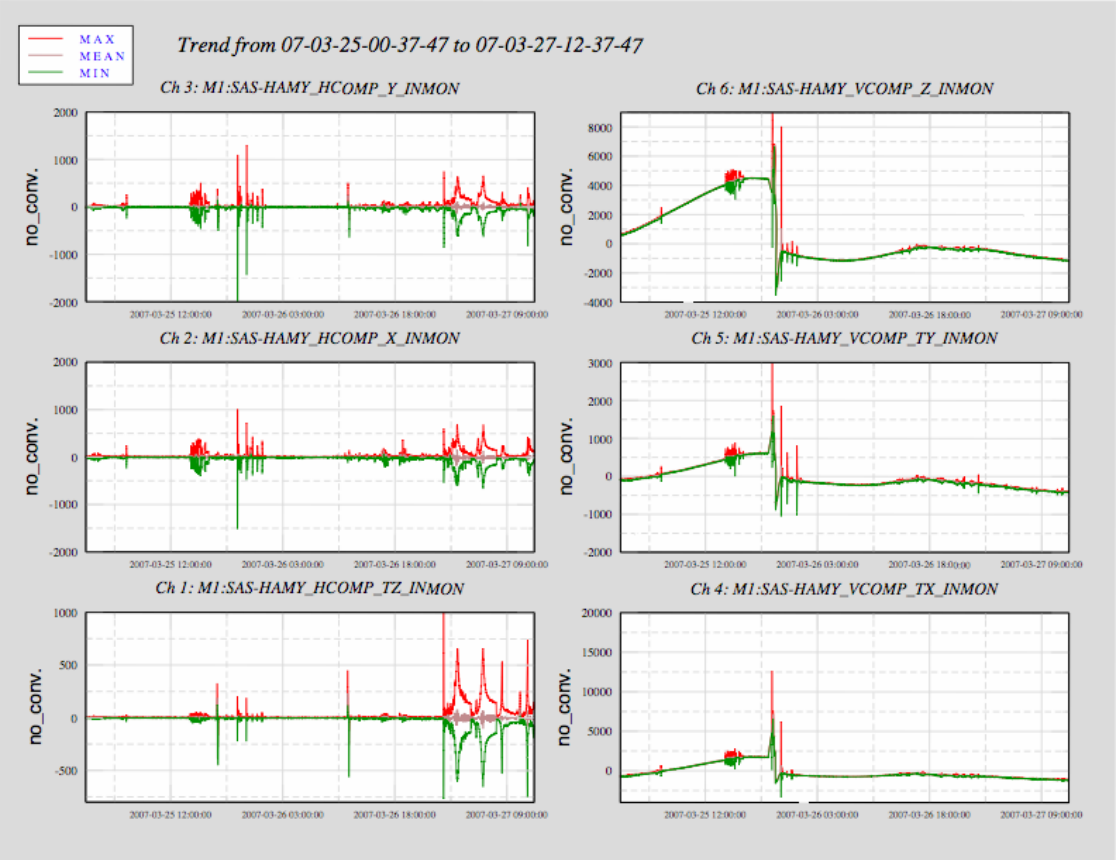

Figure A3-9: Horizontal and vertical position stability of the optical table over 2.5 days.

The table is stabilized by slow integrators in the horizontal direction while it is left free to move in the vertical direction. The oscillations are driven excitations. The initial slope in the vertical direction is blade thermalization after the adiabatic cooling during pumpdown. The break is manual table re-adjustment (using the stepper motors). The uncontrolled diurnal cycle, (±600 counts, at ~0.2 micron/count, correspond to roughly ~120 micron in Z and few hundred microradians in the two tilts) is visible after the break.

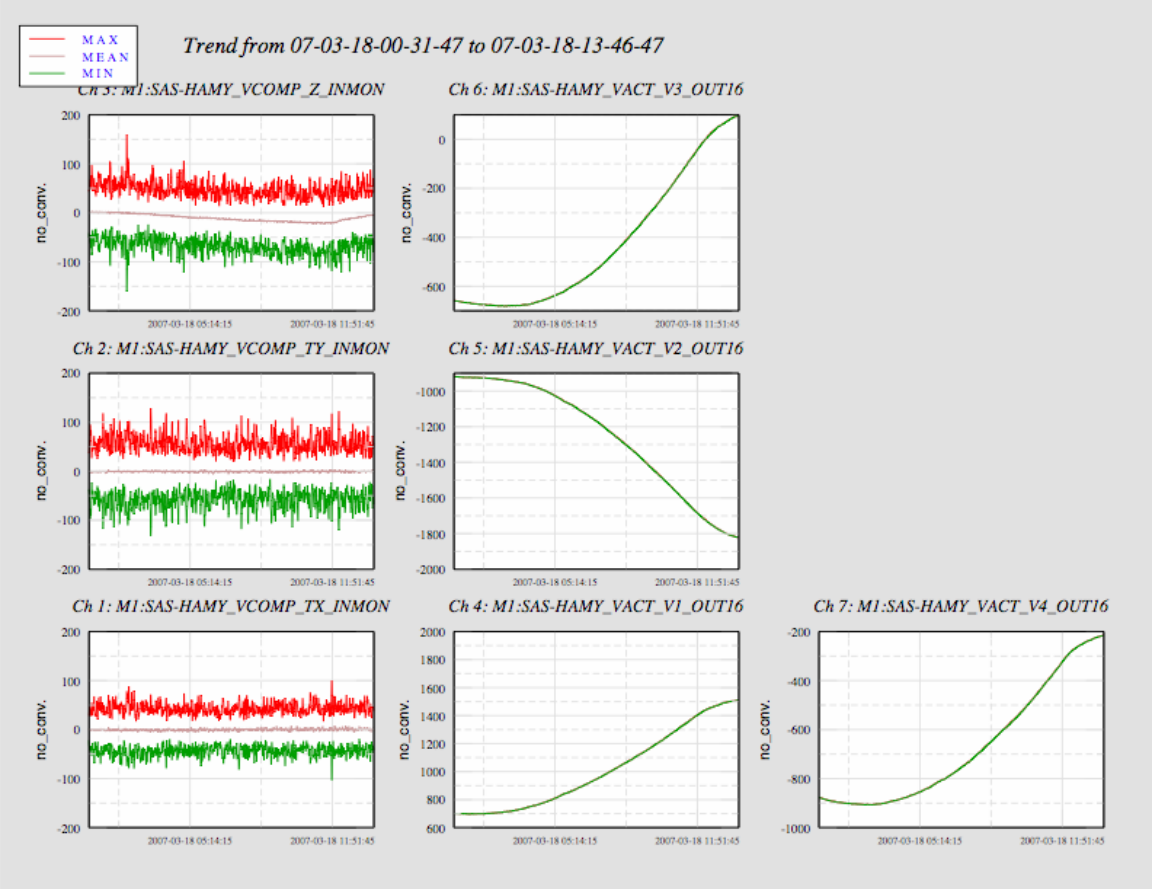

Figure A3-10. Example of overnight vertical stability with controlled vertical movement.

The overnight measurement was done with extremely weak (low bandwidth) integrators. The tilt integrators (TX and TY) are sufficient to maintain the table flat within a few counts. The vertical control integrator (Z, top left graph) is just too weak for complete thermal compensation and the table lags 25 counts (5 micron) because of the thermal drag. This test was done in air. The four graphs on the right are the commands to the four actuators (proportional to current), compensating the thermal effects. A full spread of less than 1000 counts of actuator current (railing at ±6700 counts) is used in this open door measurement. The r.m.s. spread (~75 counts, or 15 micron) shows the effect of air currents buffeting the table. It disappeared after pumping vacuum.

Parasitic positioning spring resonance damping

The correction springs are normal coil springs, quite long to get the required softness, and their high-Q violin modes are easily excited by seismic motion. These springs, 8 for the horizontal actuators, 4 for the vertical actuators, and 4 for the tilt control springs produce 16 peaks at 8 to 15 Hz. Eddy current damping of these resonances were devised and implemented on the horizontal tuning and tilt control springs. They proved completely effective on the observed 7 to 10 Hz modes.

A similar damper was also designed for the vertical direction, and parts put in fabrication. It will be installed at the next vacuum break, and is expected to have similarly good results on the observed 10 to 30 Hz modes.

GAS Filter Center Of Percussion Compensation.

The “magic wands”, used to compensate the GAS filter center of percussion (see P060044-00) have been delivered and are in the laboratory but have not been installed yet. The vertical attenuation is therefore expected to saturate at ~60 dB. After tuning (in Caltech) and installation of the wands in HAM SAS the attenuation floor should drop another 20 dB. The 60 dB saturation was observed in the transfer function.

Witness LVDTs mis-wiring.

Four Witness LVDTs measuring the relative position between the optical bench and the base structure have been added below the SAS unit. One LVDT reads the vertical displacement, one the transversal displacement, and two units the longitudinal displacement. These LVDT are run by a 10 to 20 kHz oscillator different from the one running the LVDTs in the actuation loop.

Not having a way to reach them we did not even try to engineer a signal nulling mechanism. We simply reduce the LVDT gain of these channels until the signal enters the ADC readout range. It means a reduced sensitivity and a large bias. This coarse arrangement should accent any drift of the LVDT readouts.

We incurred in a serious cabling problem. The UHV connector pinout on the LVDT box was inverted. As a result instead of routing signals on twisted pairs, the ground and one wire of the first pair was used for the first excitation signal, the second wire of the first pair and a wire of the second pair for the readback, and so on for the other 3 LVDTs.

The result is a massive cross talk that makes the witness LVDTs completely useless (see figure below, until next vent access when a short correction cable will be installed.

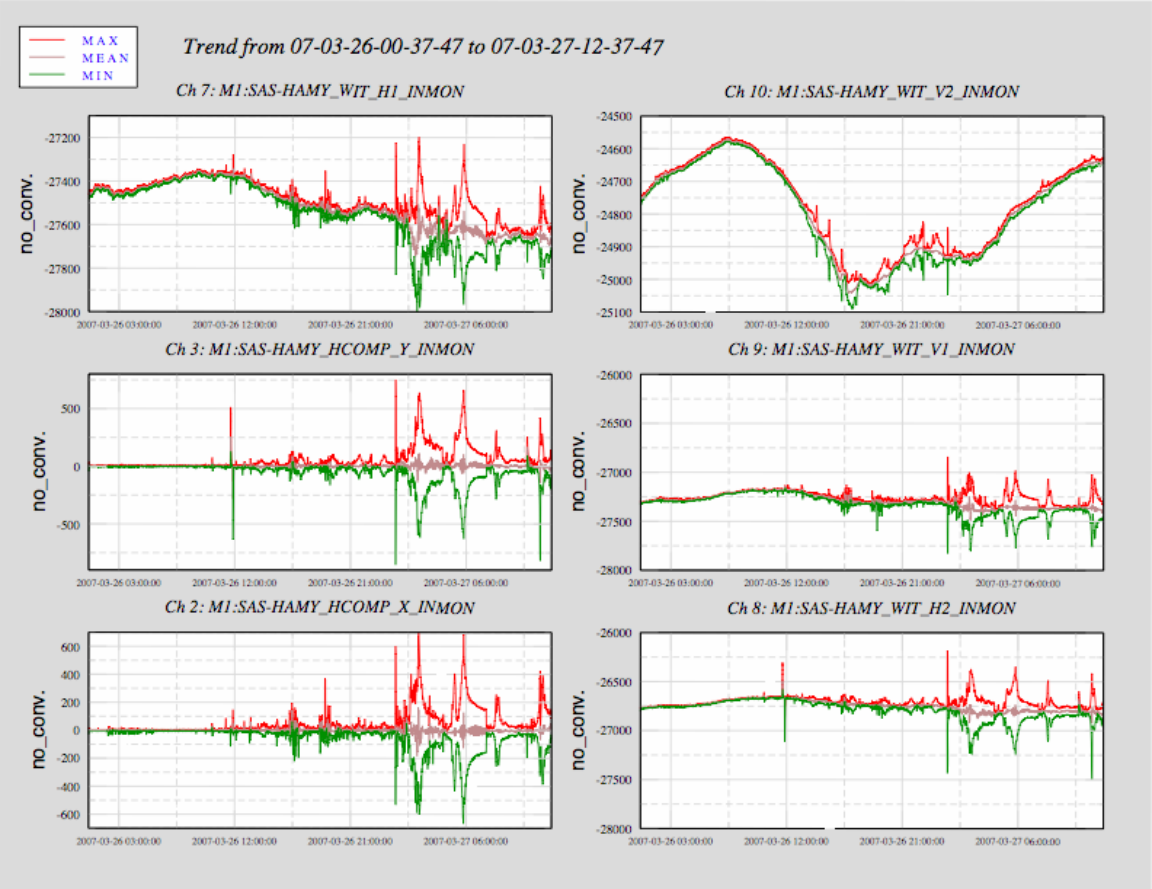

Figure A3-11. Illustration of the Witness LVDT mis-wiring induced cross talk.

The spring box in the horizontal direction is kept stable (two lower left boxes) while the vertical direction moves (vertical witness LVDT, top-right). Instead of showing flat response, the horizontal LVDTs show large cross talk with the vertical sensor.

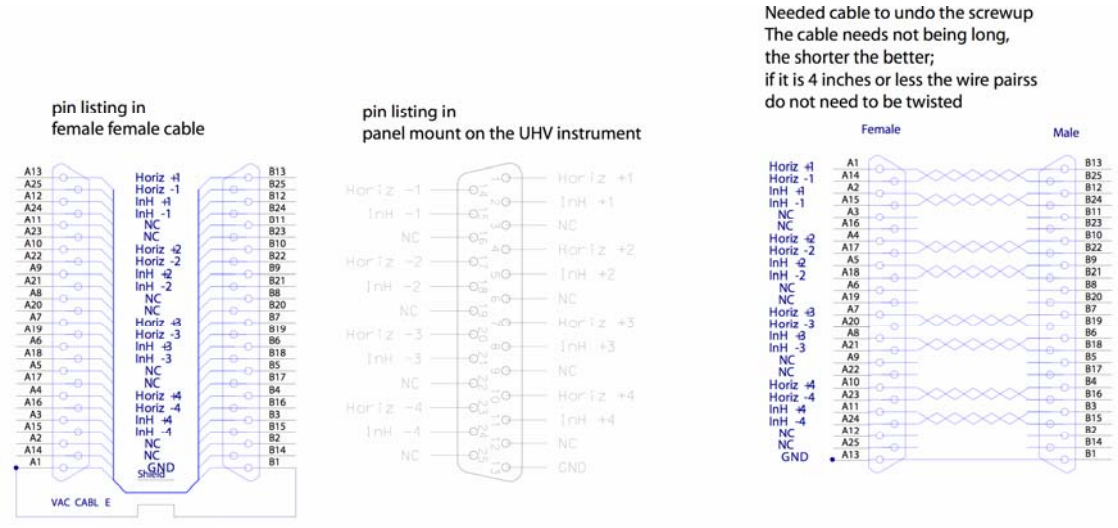

Figure A3-12. Solution of the cabling problem.

Tuning down the vertical resonant frequency.

Proper diagonalization is necessary to implement low frequency operation in all degrees of freedom. See more discussion below.

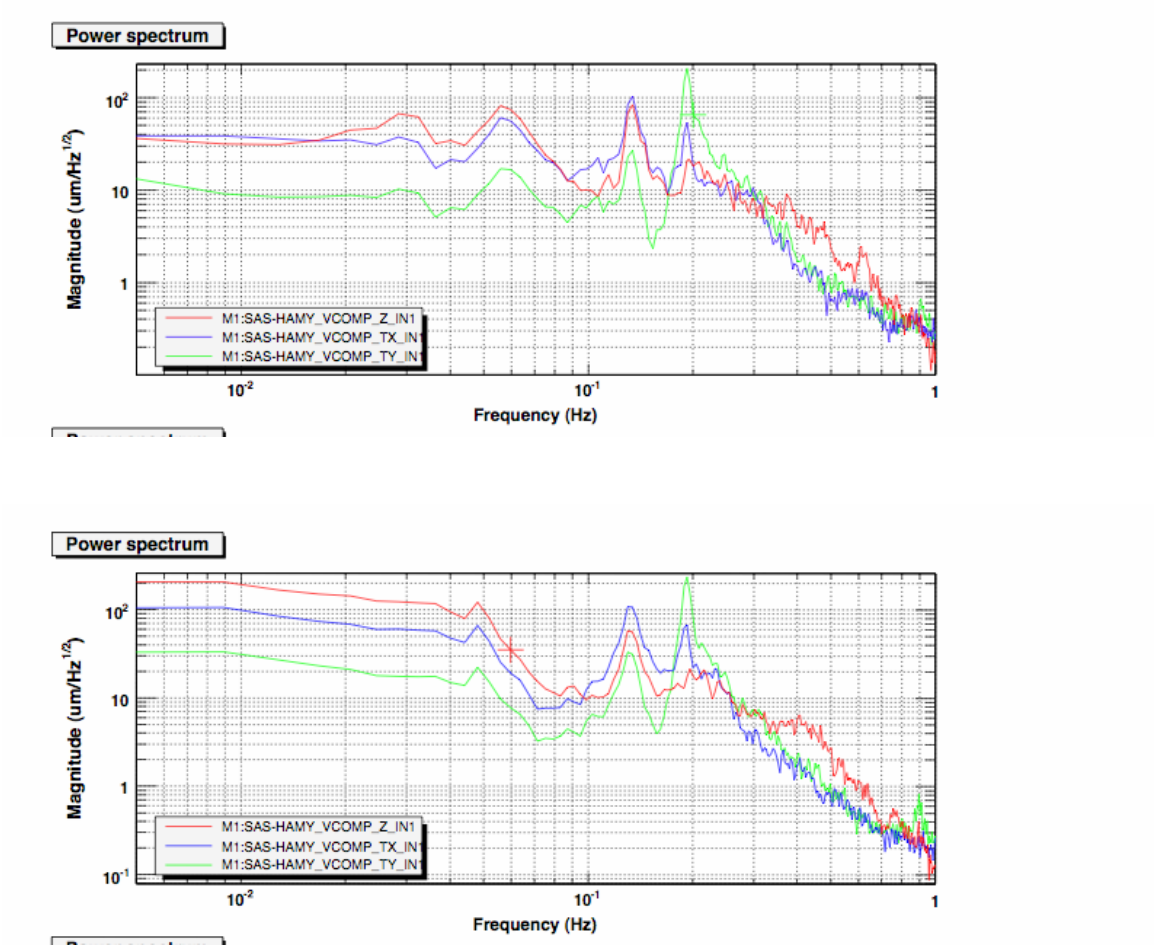

Figure A3-13. Power spectrum illustrating the effects of applying Z electromagnetic spring constant to the system. Z e.w. tilt spring gain equal 1.0 [a.u.] in the top graph and Z e.w. tilt spring gain equal 1.22 [a.u.] in the bottom graph.

The vertical resonance peak, originally at 160 mHz with no gain, was shifted down to ~55 mHz with G=1 and to ~10 mHz with G=1.22.

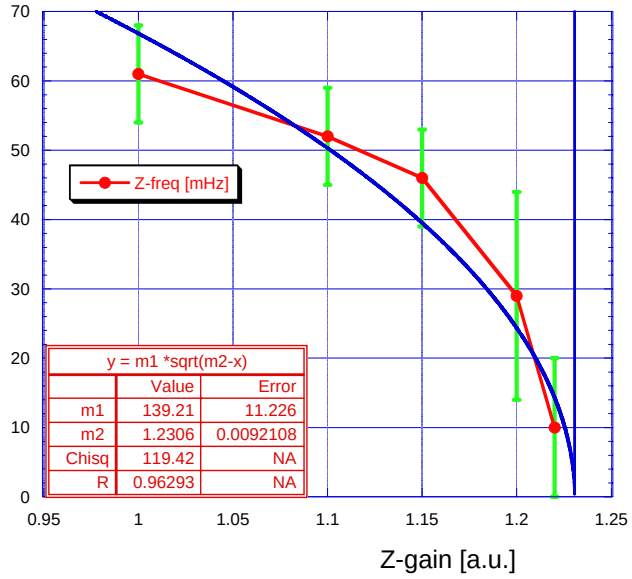

Figure A3-14. Effects of progressive gain of the e.m. Z spring.

The applied gain generated the expected reduction of resonant frequency, closely following the theoretical square root law. The error bars represent the fitted peak width, not the frequency evaluation error.

Tuning down tilt modes.

12.1 Mechanical tuning.

The tilt frequency is controlled by the mass distribution, the mechanical GAS spring stiffness over their lateral separation, and by the tilt compensation springs acting on the central roll bar. Finally, an e.m. torsional spring can be implemented and tune the tilt frequency. The asymmetric mass distribution insures that the two tilt resonant frequencies are markedly different.

The achieved tilt resonant frequencies are within the range that can be reduced by the e.m. springs. However using the e.m. springs is should always be minimized because they cannot match the reliability of passive systems and may inject noise. In addition careful diagonalization from vertical actuation must be achieved to avoid destabilizing the system.

Changing the compensation spring strength can easily change the tilt resonant frequencies, even for individual degrees of freedom. The four compensation springs are simple coil springs of various wire diameter and coil diameter. The number of turns is also used to change the spring stiffness. They are mounted at the four corners of the system and are very easy to access and replace. We have prepared compensation springs in 50% steps. We have found that 3.5 mm wire, 20 mm outer diameter, 12.5 turn springs bring the system to the point of instability, while the next available spring (8.5 turns, 50% stiffer) results in tilt frequencies of 60 mHz in one direction and 180 mHz

along the other diagonal. Availability of a wider choice of springs, and the use of different stiffness springs on the two diagonals would have allowed setting the mechanical tilt resonance frequencies at lower levels. We have ordered sets of similar springs in steps of 1 turn (9.5, 10.5 qnd 11.5 turns) and we plan to test them at a later date.

12.2 E.M. spring tuning

Only moderate reduction of tilt frequency has been achieved so far, we chose the highest tilt resonant frequency and successfully drove it down from 195 to 120 mHz, a reduction by 63% of the tilt stiffness. The process was quite predictive and followed the expected curve. The actuation authority would be more than sufficient to eliminate the remaining 25% of stiffness desired to bring the resonant frequency below 30 mHz. The progress was limited by our limited diagonalization precision. For the moment we had to interrupt the process waiting for a better diagonalization of sensors and actuators.

As a result of higher resonant frequency the resonance quality factor is too high and the low frequency attenuation performance is limited. While measuring and building better diagonalizations, we plan to limit the excitation of the tilt modes with active tilt damping.

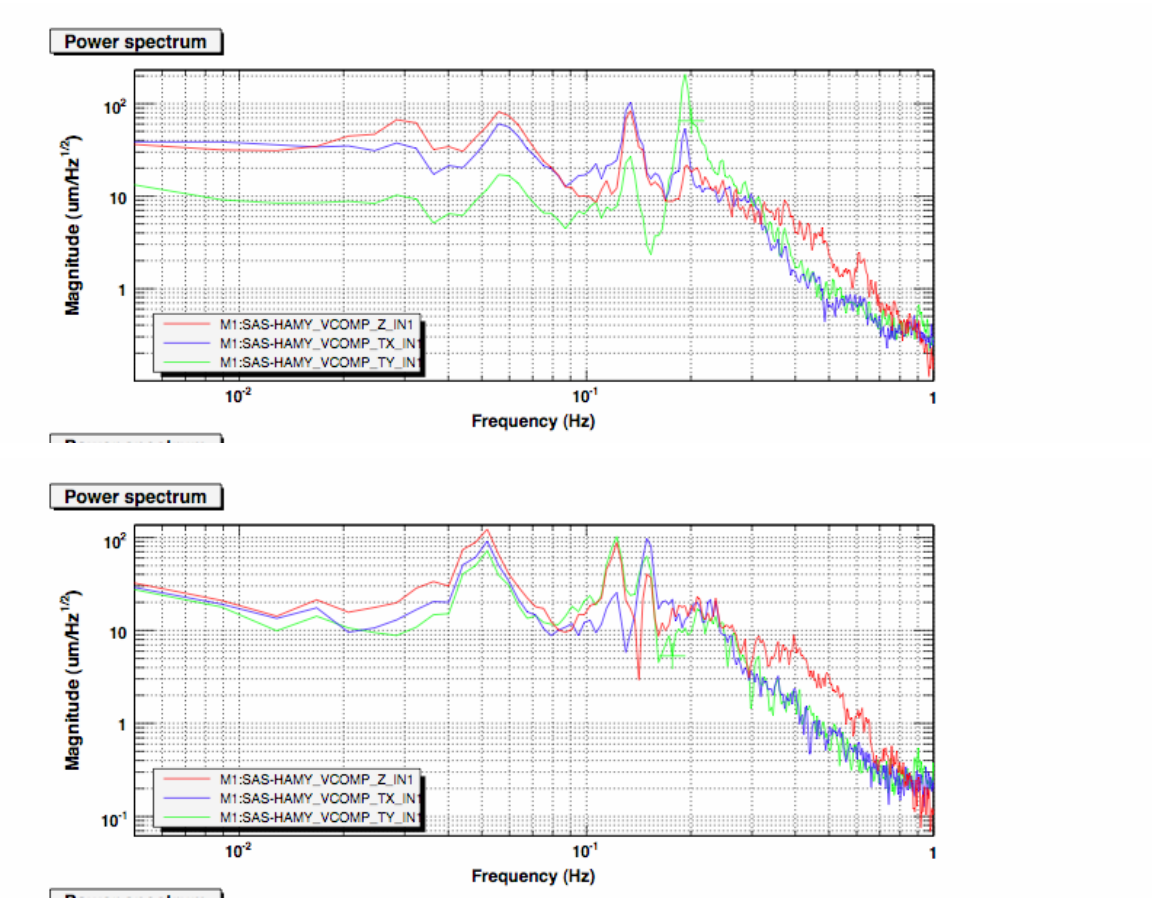

Figure A3-15. Power spectrum illustrating the effects of applying Y electromagnetic tilt spring constant to the system. No Y-tilt spring gain on top, Y e.w. tilt spring gain equal 1 [a.u.] in the bottom graph. In both cases the vertical resonance peak (52-55 mHz) was shifted down from 160 mHz using a Z e.w. spring gain equal 1 [a.u.].

The sensor and force diagonalization have been very crudely obtained, by simply adding up all sensors[(VLVDT1+ VLVDT2+VLVDT3+ VLVDT4)/2 to get the Z coordinate, using [(VLVDT1-VLVDT3)/2] for the tiltX sensor and [(VLVDT2-VLVDT4)/2] for the tiltY sensor. The green peak of the tilt Y resonance moves from 195 to 120 mHz. The effects of insufficient diagonalization are apparent. The 55 mHz vertical shifts to moves to 52 mHz and the 130 mHz Y tilt mode shifts above 150 mHz, indicating that the X-tilt actuator has a component (positive in one case and negative in the other) in both nominally diagonalized degrees of freedom. The amount of frequency shift can be used as an indicator to calculate the amount and sign of Y actuator that should be added to the X or Z actuators to improve their diagonalization.

The effects of insufficient sensor diagonalization are also apparent. The Y-tilt diagonalization in the top graph is strongly degraded by the introduction of the e.m. tilt spring. It is not that a large asymmetry or instabilities are introduced, it is that by nulling all other effects, the small mechanical asymmetries present in the system get exposed and need to be compensated.

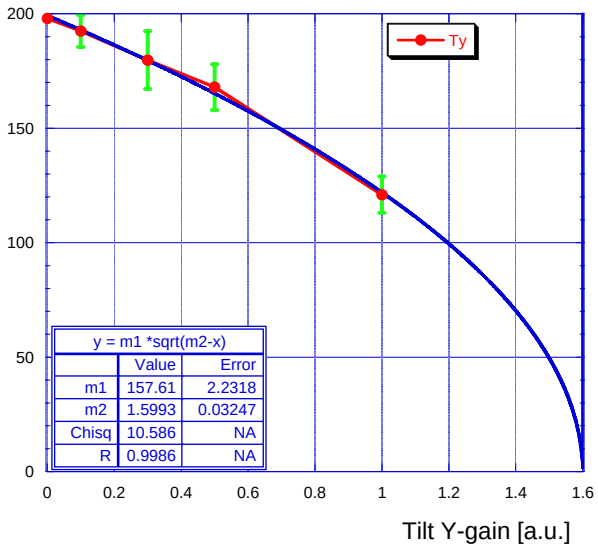

Figure A3-16. Effects of progressive gain of the e.m. Y-tilt spring.

Despite the poor sensor and actuator diagonalization, the applied gain generates the expected reduction of resonant frequency, closely following the theoretical square root law. The error bars represent the fitted peak width, not the frequency evaluation error.

Earthquake immunity.

At present we have installed a range reducing ring, that reduces the horizontal movement to ±5mm (down from ±10mm) to avoid having the horizontal actuators to act as end-stops. This reduces by a factor of 2 the amount of quake amplitude that the system accepts before hitting the end stops. Redesign of the actuator footing will solve this problem while restoring the full earthquake immunity. Of course it is not difficult to foresee the effects on the payload of quakes with excursion larger than the end-stop range.

The problem of the warped top plate, the funny modes, and the likely connection.

Originally the optical table was to be sitting on the 4 GAS spring filters on a quasi-kinematic-mount configuration (mounted on a cone, a slot and two flats instead of one, taking advantage of the GAS elasticity to guarantee the fourth mechanical contact while preserving positive transversal positioning).

The requirement of the addition of the witness LVDTs between the optical table and the base structure (for the LASTI prototype only) forced the last minute addition of an intermediate plate holding the four LVDT primaries. This turned out to be a positive design change because it eliminated all needs of machining the old tables, that can now be recycled "as is". Additionally there is an important simplification of the insertion procedure. Not having to raise the optical table so that the kinematic mount pilllars clear the spring box top plate before lowering it onto the kinematic mount, it is possible to insert the table at, or even a few mm below its intended working level The GAS filters are released after the table is in its working location to pick up the load. This is potentially very useful to install a completely populated and pre-aligned bench.

The mechanical problem originated from the fact that we re-cycled a rejected aluminum plate from a failed base structure construction. Unfortunately this plate had been planed on one side in its previous failed machining, and during the final bakeout it warped. The warp straightened itself out under the weight of the optical bench, but its deformation under load forced at least one GAS filter keystone to bend 10 to 15 mradians, and the associated filter (filter No. 1) to work crooked. Filter 1 is the one with the cone of the kinematic mount; The problem may be present to a smaller extent also on the other filters. The problem manifested itself when we found that the actuator of filter 1 was rubbing against the LVDT secondary.

The problem was solved taking advantage of the play of the screws to regenerate some clearance, and we took note to change the warped plate whenever the system would be overhauled. We though that the problem had no other consequences.

Although not proven, it is likely that the problem is at the root of a strange table behavior now that we are pushing SAS to lower frequencies. We expected that the vertical movement would diagonalize well from the two tilts, and that the two tilts would be almost degenerate. To our surprise we found that there is a lot of cross talk between the Z movement and the X tilt. While the Y-tilt diagonalize well, as expected. The expected X tilt involves the movement of GAS spring 1 going up and down while GAS spring 3 goes down and up, while 2 and 4 do not move.

We are fairly confident that this is not generated by rubbing (we inspected the rubbing LVDT and see ~1/2 mm clearance and all free oscillations seem normal).

We are also confident that this is not generated by original differences between the four GAS filters because they had been equalized to a very high degree, see table below.

Filter	Frequency [mHz]	Optimal Load [Kg]	Height [mm]
A	192	276.21	19.46
B	180	275.42	19.95
C	188	276.34	20.15
D	180	276.45	20.03

We suspect that, now that all other forces null each other, the GAS filter asymmetry generated by the warped plate causes the unexpected mode mixing. Our belief stems form the fact that the crooked GAS filter is directly involved in the tilt mode that mixes with the vertical motion.

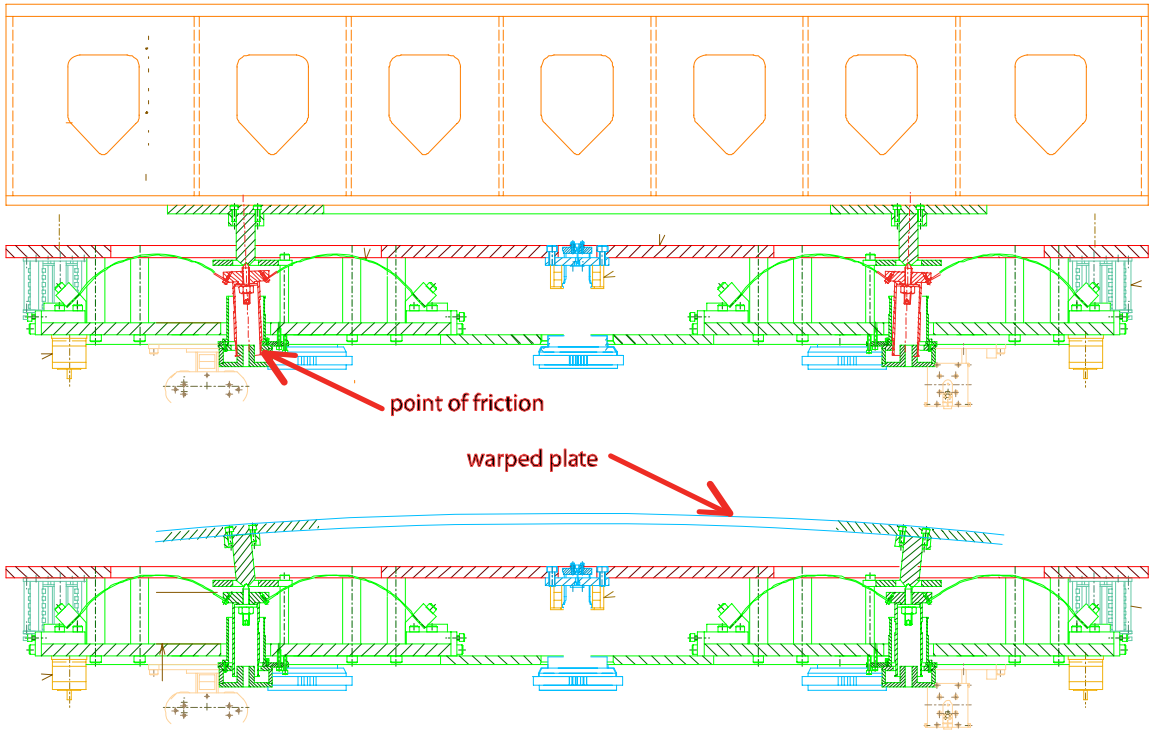

Figure A3-17. The warped plate (exaggerated in bottom sketch) straightened up under the load of the table but forced at least one GAS filter to work crooked and generated a friction point (top sketch).

This asymmetry complicates the control and frequency tuning problem and is expected to slow down the frequency tuning process.

The figure shows the strength required from a first attempt of a modal actuation matrix, and illustrates the deviation from the geometrical diagonalization due to the observed modal cross talk.

The actuators diagram in figure are well diagonalized (excite only the mode of interest and leave the other modes not excited).

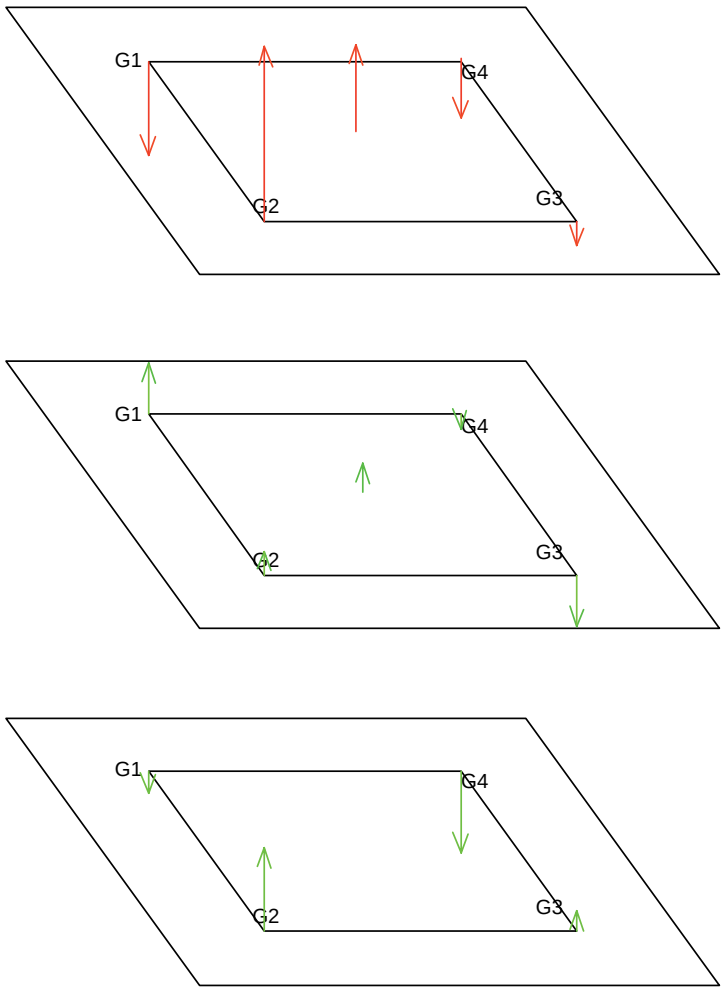

Figure A3-18. Diagram of forces applied on the four vertical actuators from a first attempt of modally diagonalized actuation matrix. The vertical component, when present, has been factored out and shown as a separate arrow at the center (force on each actuator, to have the actual vertical force the central vector must be multiplied by 4).

While the bottom virtual (tilt) actuator is well diagonalized from the vertical direction, sizeable cross talk is visible between the vertical and the other tilt actuator.

Walking test.

The stability of optical bench was monitored during the early morning, and shortly later while cabling around and over the HAM chamber to install thermocouple probes.

The minute-trends over the time covering the two periods show a smooth slope in the current requests to maintain level and altitude. This request is probably due to room temperature drifts.

The first half of the time span shown in the graph is quiet time before people arrived in the lab, then activity starts and tY changes drift direction. It is a tilt. We note that the Z movement does not significantly change trend.

The last 40 minutes show the effect of people going around the chamber and, in the last few minutes, the effect of climbing on a pier.

The following figure show seismometer and geophone spectra (randomly chosen) during the quiet time, and while people crawl around.

The larger mechanical disturbance injected on the HAM chamber structure penetrates the HAM SAS, but the optical bench easily maintains its position relative to its base structure.

Note that the position is maintained with respect to the base structure, which rests on the piers. If moving on the piers results in a movement of the base structure resting on them, the SAS system simply tracks it.

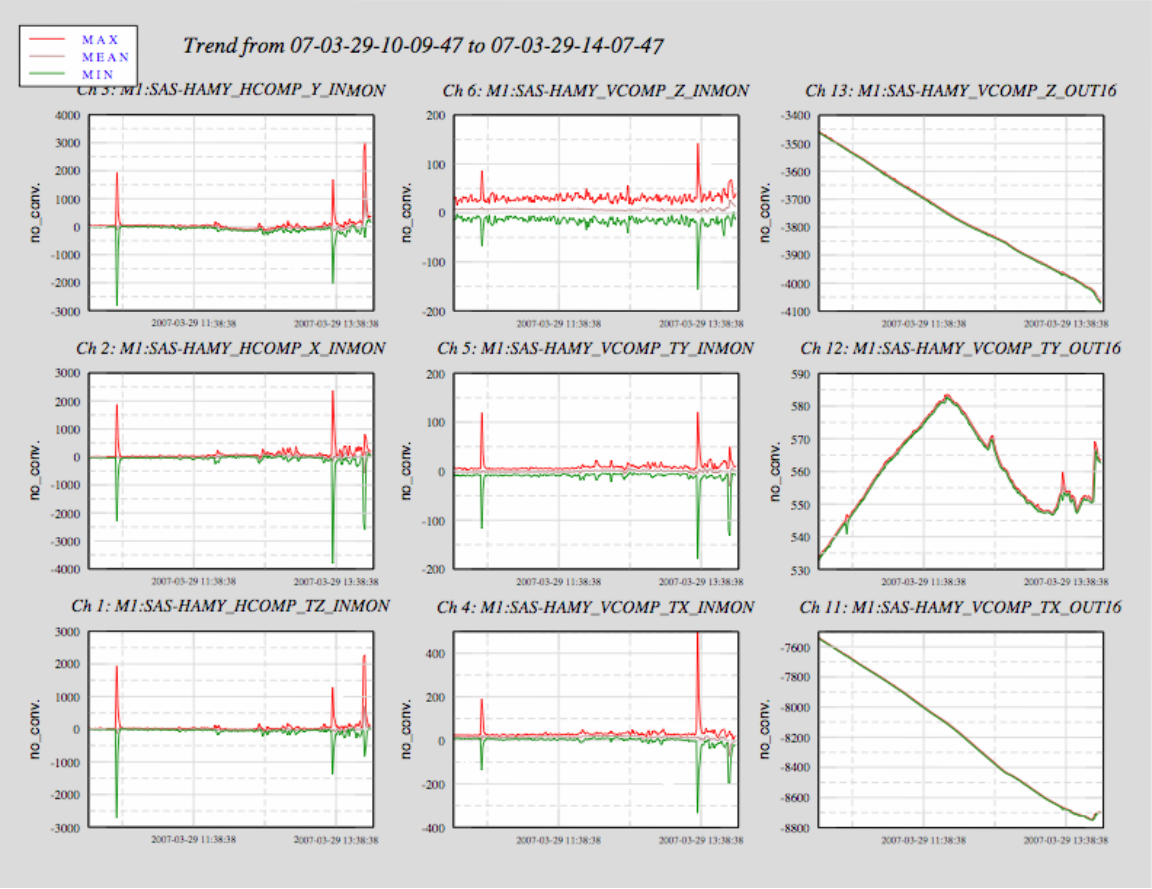

Figure A3-19. Position monitors over a ~2 hours overnight period with integrator loops maintaining the positions in the six degrees of freedom. The three graphs on the left monitor the horizontal stability, the three middle graphs monitor the vertical stability and the three graphs on the right monitor the modal actuator (i.e. the actuator current request necessary to maintain the position). A seismic event appears in the first ¼ of an hour; half way through the graph time span people start moving in the lab, something, possibly a movement of mass or a truck parked outside, suddenly changes the ground tilt drift direction and changes the current request to maintain the TY leveling (and to a much smaller extent the TX leveling. In the last ¼ of the time the cabling activity starts, including in the last few minute climbing on a pier.

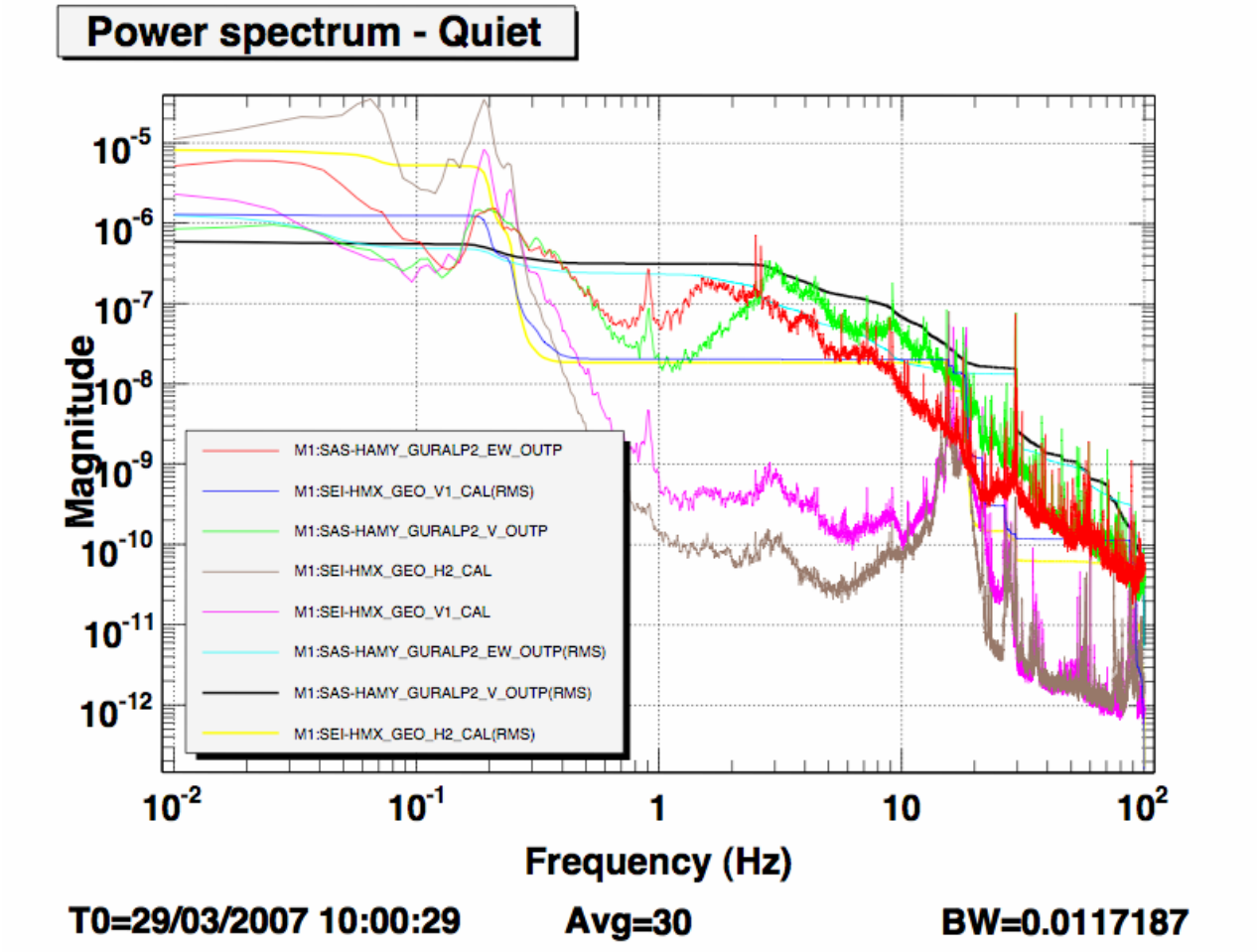

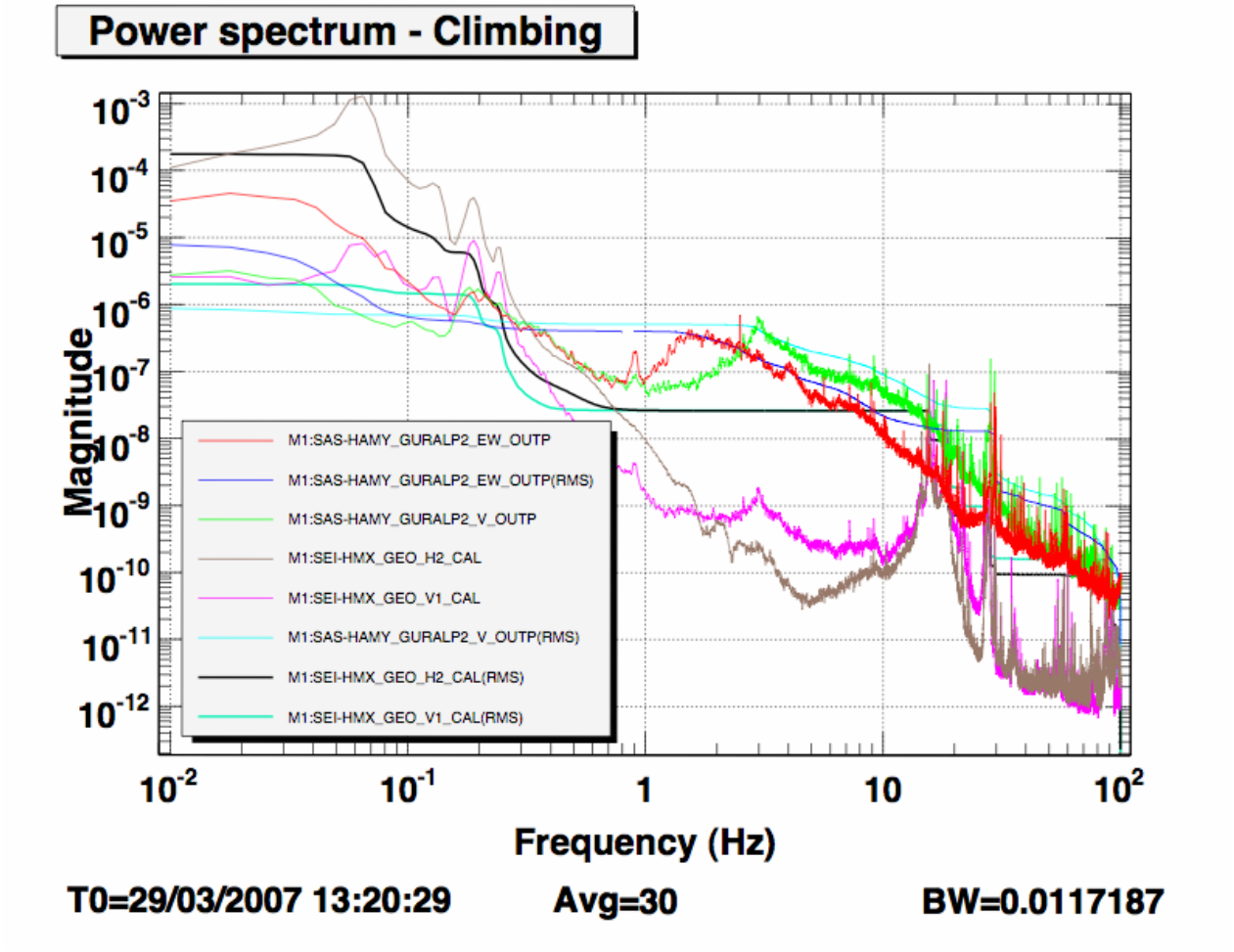

Figure A3-20: Power Spectra Density of Seismometer on ground and geophones on the optical bench power spectra before (top graph) and during cabling activity around and on the HAM chamber (bottom graph). Mechanical noise is injected on the optical bench by the installation activity.